International TOVS Study Conference-XXI Proceedings
Comparison of the simulated microwave cloudy radiances using ARTS and RTTOV-SCAT

Victoria Sol Galligani [1,2,3,4]
[1]Centro de Investigaciones del Mar y la Atmofera (CIMA),
[2]Instituto Franco Argentino sobre Estudios de Clima y sus Impactos (UMI IFAECI)/CNRS,
[3]CONICET, [4]Universidad de Buenos Aires, Buenos Aires, Argentina

Abstract

This paper discusses ongoing work to compare the fast operational model RTTOV with the physics-based, research model, ARTS under cloudy conditions to intercompare their scattering solvers. The simulations discussed in this paper correspond to simple scenarios where clear-sky, rain-only cloudy and snow-only cloudy conditions from a realistic deep convection case are modelled. The simulation discussed analyse the behaviour of the radiative transfer models to different parameters, such as the scattering properties, the zenith angle, or the cloud mass contents. Under clear sky conditions where both ARTS and RTTOV use the same water vapour absorption model, differences were shown to be below 1.5 K for nadir simulations. An analysis of the sensitivity of these simulations to zenith angle showed larger differences for zenith angles higher than $\sim$45 degrees. For cloudy conditions, the sensitivity of the ARTS simulations to MC min_iter, and RT4 nstreams and quadrature type were tested for rain-only and snow-only simulations, using the soft sphere approach and 3 habits from the Liu [2008] DDA database for the latter. Using the soft-sphere approximation a strong sensitivity in the differences between RTTOV and ARTS cloud signals were shown as a function of zenith angle, but the these differences remain constant with snow water level fraction. The contrary is observed using DDA habits. There is no zenith angle sensitivity in the differences between RTTOV and ARTS, but there are differences as a function of snow water level fraction for all DDA habits.

1 Introduction

Radiative transfer models are used in numerical weather prediction (NWP) as observation operators during assimilation. In order to assimilate passive microwave radiances in an all-sky scenarios, an improvement in our understanding of the scattering properties of frozen hydrometeors is essential. At high microwave frequencies, frozen hydrometeors significantly scatter radiation, and the relationship between radiation and hydrometeor populations becomes very complex. The main difficulty in cloudy microwave remote sensing is correctly characterizing this scattering signal due to the complex and variable nature of the size, composition and shape of frozen hydrometeors. The scattering solver approximations used in fast operational radiative transfer models are also important sources of errors. In that respect, this paper discusses the first steps taken on an ongoing comparison between the very fast radiative transfer for the TIROS Operational Vertical Sounders (RTTOV) and the research Atmospheric Radiative Transfer Simulator (ARTS). It is important to compare the simulation results from fast scattering model solvers to external models that may be more robust or accurate. This exercise also allows to develop an understanding of the systematic errors, or deficiencies, that may be presented in any given model. Hence, such radiative transfer model intercomparisons, covering both clear-sky and cloudy-sky, are considered to be of considerable importance by the radiative transfer community. The present work compares a fast operational model like RTTOV with a physics-based model like ARTS that includes full scattering solvers and another fast scattering solver.

The simulations discussed in this paper correspond to simple scenarios where clear-sky, rain-only cloudy and snow-only cloudy conditions from a realistic deep convection case are modelled. These are simple, yet key comparisons that must be discussed before analysing more complex scenarios, in order to understand the behaviour of the models to different parameters, such as the scattering properties, the zenith angle of simulations, or the cloud mass contents. This paper is structured as follows: Section 2 provides a brief account of the two models compared. Section 3 describes how the comparison was undertaken by describing the configuration of the simulations. Section 4 provides an account of the model comparison and finally, Section 5, provides a summary and future ongoing work.

2 The radiative transfer models: RTTOV and ARTS

The radiative transfer model for TOVS, RTTOV, was originally developed at ECMWF in the early 90s Eyre [1991] for the TIROS Operational Vertical Sounders (TOVS). Since then, RTTOV has undergone many developments and today RTTOV v12 is used operationally to assimilate visible, infrared and microwave radiances. RTTOV-SCATT is a component of the RTTOV package designed for cloudy-sky conditions with the aim of assimilating all-sky condi-

tions Bauer et al. [2006]. RTTOV achieves its speed by using pre-calculated coefficients for several predictors, based on a training set of monochromatic transmittances, that translate the atmospheric profiles into polychromatic transmission for select channels at some atmospheric profile levels. On the other hand, the Atmospheric Radiative Transfer Simulator (ARTS, Eriksson et al. [2011]) is a much more flexible, research model that can be used for monochromatic line-by-line calculations anywhere within the microwave to the infrered spectral range. ARTS is a physics-based model and therefore much slower than RTTOV, for example, it is a line-by-line model that calculates absorption from a spectral line database for every level of the input atmospheric profiles. In terms of radiative transfer under cloudy-sky conditions, ARTS provides several scattering solvers.

RTTOV assumes a plane-parallel and azimutally symmetric atmosphere to calculate satellite radiances employing the Doubling-Adding Method and the Eddington approximation given an atmospheric profile of pressure, temperature, variable gas concentrations, cloud hydrometeor concentrations and surface properties. The water vapour and oxygen RTTOV absorption coefficients are precalculated according to the Liebe [1989] absorption model. RTTOV then interpolates the input profile data onto fixed coefficient levels, calculates the optical depths on the coefficient levels and then interpolates the optical depths back onto the input pressure levels. Note that the present ongoing work uses the recently available band-correction coefficients. Optional trace gases that can be included in the simulations are ozone, carbon dioxide, carbon monoxide, methane, sulphur dioxide and nitrous oxide, but are here turned-off for simplicity. The simulations presented in the present work for both ARTS and RTTOV include only oxygen and water vapour gas absorption. In the present ongoing work ARTS simulations are conducted using one dimension, where the atmosphere is described as being spherically symmetric, and different absorption models are tested for water vapour: the Rosenkranz [1998], the Liebe [1989] and the Liebe et al. [1993] model. In terms of the surface properties, both models are configured with the same surface temperatures and the same simple specular reflection surface emissivities for the comparison.

The additional variables needed by RTTOV-SCATT for RT calculations under cloudy conditions include level pressure and cloud hydrometeor particles: information of the n-levels of cloud cover (0-1, here assumed to be 1 in the levels where hydrometeors are present for consistency with ARTS) and the mixing ratio of the cloud hydrometeor particles included in the simulation. For cloud scattering properties, RTTOV-SCATT uses a pre-calculated scattering coefficients lookup table and allows only a limited number of hydrometeors (see section below). This lookup table can be pre-calculated under a fixed number of parameters such as different mass-size relations or particle size distributions. RTTOV-SCATT then uses Delta-scaling Joseph et al. [1976] on the optical parameters accounting for the highly asymetric phase function in the presence of strongly scattering atmospheres. Finally, cloudy-sky brightness temperatures are obtained by RTTOV by linearly combining radiances of clear and cloud sky by applying a two-independent column (2-IC) approach where $T_{allsky} = (1-C)T_{clear} + CT_{cloudy}$. C is the effective cloud fraction in the vertical profile.

On the other hand, ARTS includes several modules to solve the radiative transfer equation in cloudy-sky conditions, of which the Monte Carlo (MC) algorithm [Davis et al., 2005] and the integrated RT4 scattering solver developed by Frank Evans [Evans and Stephens, 1995] are used in the present ongoing comparison. Comparing RTTOV-SCATT with these two modules is an interesting task as the three models cover different levels of code complexity. ARTS allows a larger degree of flexibility than RTTOV when calculating the hydrometeor optical properties as these are explicitly defined by the user. The additional variables needed for ARTS to run the scattering solvers include profiles of the hydrometeor mass content, the particle size distribution and the single scattering properties. Special care is taken such that the same scattering properties are used in both ARTS and RTTOV (see section below).

ARTS allows the user to set the minimum number of allowed iterations (hereafter min_iter) in MC simulations for a target precision of, in this study, 0.1 K in standard deviation. The RT4 scattering solver uses the doubling-adding method and inside the model the radiation field is represented with a Fourier series in azimuth angles and the zenith angles are discretized using a numerical quadrature. The quadrature type and the number of quadrature angles (or nstreams) depend on the desired accuracy. These variables: min_iter, nstreams and quadrature type are tested in comparison with RTTOV-SCATT.

3 Simulation settings

The atmospheric data used in this comparison belongs to the Chevallier-91L dataset [Chevallier et al., 2006], more specifically to the deep convection scenario. Figure 1 shows the temperature and water vapour profiles used. Using these atmospheric profiles, clear-sky simulations are run using both RTTOV and ARTS under fixed surface emissivities: 0.6 for ocean emissivities and 0.9 for land emissivities (specular reflection). Simulations are carried out for the Microwave Humidity Sounder (MHS). MHS has channels centered around 89.0, 157.0, 183.311$\pm$1,3 and 190.311 GHz. The same sensor spectral channel offset and bandwidth used in RTTOV (see RTTOV User Guide for more details) are used in ARTS. As mentioned in the introduction, three different water vapour abortion models available within ARTS are tested: PWR-98 [Rosenkranz, 1998], MPM89 [Liebe, 1989] and MPM93 [Liebe et al., 1993]. The sensitivity of each model to zenith angle is also tested by running clear-sky simulations for different observation angles.

To compare RTTOV-SCATT with the scattering solvers provided by ARTS, the rain and snow profiles from the Chevallier-91L deep-convection scenario shown in Figure 2 are included to the above mentioned simulations.

The present analysis focuses on the most simple comparisons in order to build up a good understanding of the behaviour and sensitivity to cloud variables of the different models in the context of further ongoing work. For this reason, in the present work, the rain and snow profiles shown

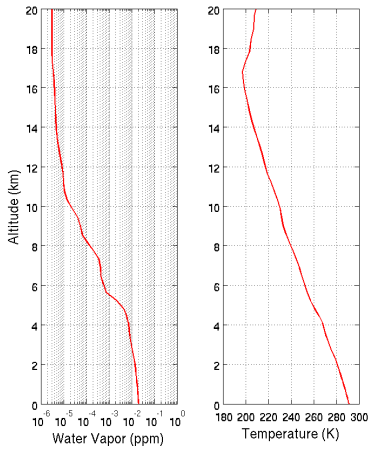

Figure 1: The temperature and water vapour profiles used in the present comparison. They belong to the Chevallier-91L deep-convection scenario [Chevallier et al., 2006].

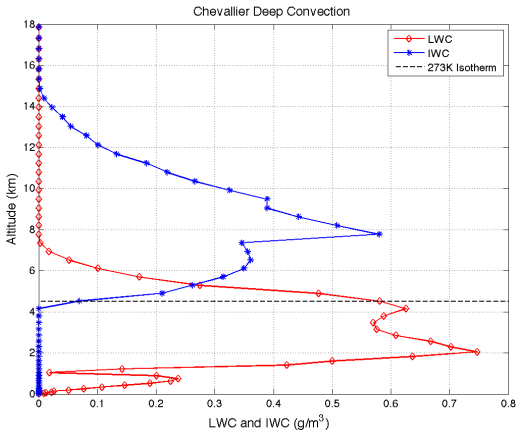

Figure 2: The rain and snow profiles used in the present comparison. They belong to the Chevallier-91L deep-convection scenario [Chevallier et al., 2006].

in Figure 2 are simulated one by one, hence two different cloudy-sky scenarios are explored: rain-only and snow-only simulations. The aim of the simulation configurations is to maintain consistency between RTTOV-SCATT and ARTS. As described in Section 2, RTTOV-SCATT requires the profiles of cloud cover and the mixing ratio of the cloud hydrometeor particles included in the simulation. Cloud cover is assumed to be either 0 or 1 in each layer, where cloud cover is 1 where the mixing ratio is > 0, and the mixing ratios are supplied by the Chevallier-91L deep-convection scenario. Similarly, the effective cloud fraction in the 2-IC equation presented in Section 2 is set to 1 where the column integrated hydrometeor mass is > 0. This is to establish consistency with ARTS where no treatment for sub-grid cloud variability is specified.

Since the generation of the bulk optical properties is computationally demanding, RTTOV relies on pre-calculated scattering coefficients for each hydrometeor type as a function of temperature, frequency and mass content. Given the mass content of each hydrometeor type present in the layer, the final bulk optical properties of the layer are obtained from the coefficient tables. Unlike RTTOV, ARTS requires profiles of hydrometeor mass content, particle size distribution and the single scattering properties to be explicitly set by the user. Bulk scattering properties are then calculated within ARTS.

Special care is taken such that there is consistency in the bulk scattering properties used in both ARTS and RTTOV. The RTTOV cloud scattering coefficients were calculated with the same parametrizations as those used in ARTS simulations. For the rain-only simulations, mie theory is used to calculate the scattering properties of rain spheres that follow $N_r(D) = N_o exp(-\lambda D)$, where $\lambda = (\pi N_o \rho_w / q_r)^{1/4}$, $N_o = 8E6$, ρ_w is the water density, and q_r is the rain mixing ratio. In RTTOV, by default, the PSD and the SSPs are calculated for 100 different diameters equally spaced between 0.1mm - 1mm. ARTS simulations were run to test the sensibility of using 30 or 100 diameter intervals between the same dmin and dmax. No considerable impact was observed and the simulations shown here correspond to the 30 diameter intervals. The bulk scattering properties used by RTTOV and those used as inputs in ARTS were compared and good consistency was observed (not shown). Similarly, the snow single scattering properties are calculated using mie theory. Frozen particles are assumed to be made up of ice inclusions in an air matrix, with the dielectric properties combined according to the Fabry and Szyrmer [1999] mixing formula. This is known as the soft-sphere approximation. The DDA Liu [2008] scattering database is also tested in the present study. Geer and Baordo [2014] have added into RTTOV-SCATT the facility to use optical properties for non-spherical hydrometeors from this database, available since RTTOV v11. Only three habits of the 11 habit database are discussed: the 6 bullet rosette (6b. ros), sector and dendrite habits. The snow hydrometeors in the simulations follow $N_s(D) = N_o exp(-\lambda D)$, where $\lambda = (\pi N_o \rho_w / q_s)^{1/4}$, $N_o = 4E6$, ρ_s is the snow density (for the soft sphere approximation ρ_s is 100 kg/m^3), and q_s is the snow mixing ratio. In terms of the number of diameters with which the PSD is discretized, special attention needs to be paid for the DDA Liu [2008] habits. For the soft sphere approximation used with mie theory, the same conclusions drawn for rain-only simulations apply and the simulations shown correspond to 30 diameter intervals. On the contrary, special attention is required for the DDA habits. RTTOV coefficient files are built by running the code distributed by the Liu [2008] database to retrieve the scattering properties for 100 diameters between 0.01 and 2 cm. However, ARTS runs the DDA simulations with a special version of the Liu [2008] database. This database is composed of the single scattering properties of an ensemble of particles of size Dmax, where Dmax for the 6b. ros and dendrites are for example 0.0050, 0.0100, 0.0200, 0.0300, 0.0400, 0.0500, 0.0750, 0.1000, 0.1500, 0.2000, 0.2500, 0.3000, 0.3500, 0.4000, 0.5000, 0.6000, 0.7000, 0.8000, 0.9000, 1.0000 cm. To keep

consistency in the RTTOV and ARST bulk scattering properties, the ARTS derived bulk properties use the diameters in the database distributed with ARTS, despite using a much coarser diameter population in the ARTS simulations. Despite this difference in the PSD population, good consistency is found in the bulk scattering properties (not shown).

The following subsections examine the clear-sky comparisons first, followed by the rain-only and snow-only simulations. For these scattering scenarios, the simulations here presented examine the sensitivity of the simulations to zenith angle and hydrometeor mass content, as well as to the scattering solver settings described in Section 2: min_iter in MC and, nstreams and quadrature type in RT4.

4 Model comparison

Clear-sky conditions

Figure 3 shows the ARTS and RTTOV MHS clear-sky simulations at nadir for ocean emissivities (0.6) using the configuration described above for three different absorption models with ARTS: MPM89, MPM93 and PWR-98. Note that as described above, RTTOV uses the MPM89 model. As shown, the brightness temperature differences between the radiative transfer models for the absorption MPM89 model are below 1.5 K. The largest differences are observed when the PWR98 model is used, with differences of up to 5.5 K at 89 GHz. Focusing on the MPM89 model, the differences at nadir between ARTS and RTTOV have similar orders of magnitude for other Chevallier profiles tested (not shown). These simulations were also tested with different RTTOV absorption coefficient interpolation methods and no relevant changes were observed.

Note that Figure 3 shows that the largest differences using the MPM89 model are found for the water vapour channels, which also had the largest difference in the optical depth and level transmittance calculations, specially in the lower levels of the water vapour channel. The ARTS-MPM89 (RTTOV) total optical depths are 0.49 (0.49), 1.75 (1.76), 43.38 (15.75), 23.1 (22.18) and 7.37 (8.23) for 89, 157, 183.311+0.981, 183.311+2.9790 and 190.311 GHz respectively. The RTTOV optical depths diverge from those modelled by ARTS in the water vapour sensitive channels, mainly because the transmittances in the lowest levels of the atmosphere in RTTOV are not constrained by the regression scheme. The levels that do not affect the sensor TOA radiance, i.e., those levels that are not sensitive to the channel, are excluded from the RTTOV training scheme. For example, the ARTS and RTTOV transmittances at 183.311+0.981 GHz match up well down to ∼5km (not shown) because below these layers the satellite is no lower sensitive to the atmosphere. Above these layers, RTTOV is doing a good job at parametrising the optical depths.

Figure 4 shows the difference between RTTOV and ARTS-MPM89 simulated brightness temperatures as a function of zenith angle for both land emissivities (solid line) and ocean emissivities (circle markers). At window channels (89 and 157 GHz), differences are observed between ocean and land emissivity simulations, as expected. As discussed above for nadir simulations, the largest differences are found at 190

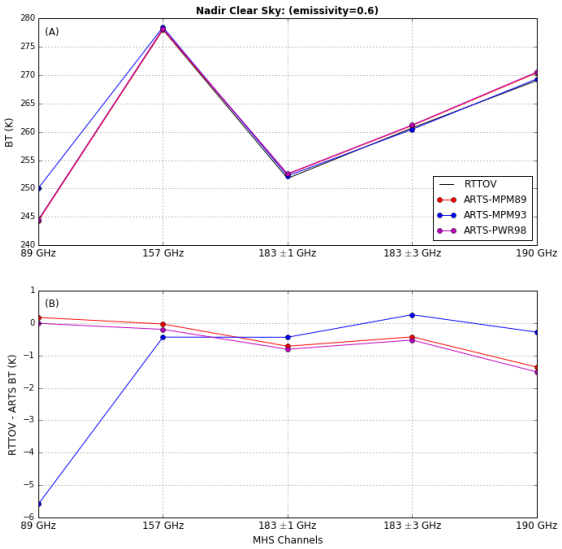

Figure 3: (A) Nadir clear-sky simulated brightness temperatures for ocean emissivities (0.6) at MHS channels using RTTOV, ARTS-MPM89, ARTS-MPM93 and ARTS-PWR98 for the clear-sky Chevallier-91L profile presented in Section 2; (B) The difference in the simulated brightness temperature by RTTOV and the different ARTS absorption models.

GHz, which is also shown in Figure 4 for other zenith angles. In general, RTTOV and ARTS-MPM89 differences increase with zenith angle, specially above ∼45 degrees. This is discussed below for cloud-sky conditions too.

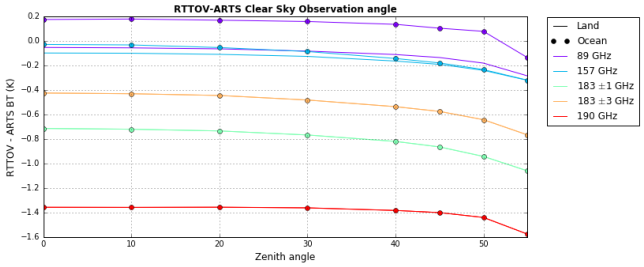

Figure 4: Differences in the clear-sky simulated brightness temperatures for ocean and land emissivities (0.6 and 0.9) at MHS channels as a function of zenith angle using RTTOV and ARTS-MPM89 for the clear-sky Chevallier-91L profile presented in Section 2.

Cloud-sky conditions

This section examines the cloud-sky simulations. ARTS simulations are run with the MPM89 water vapour model as good consistency was shown with this absorption model

for clear-sky simulations in the section above. As mentioned in Section 3, the sensitivity of the ARTS simulations to MC min_iter, and RT4 nstreams and quadrature type were tested in the present study for the rain-only and snow-only simulations. ARTS-MC simulations were run with different min_iter values for a target precision of 0.1 K in standard deviation, with values ranging from 100 to 2400 min_iter. RT4 simulations was run with Gauss-Legendre and double Gauss quadrature, with 4, 6, 10, 16, 20 and 30 nstreams. Although rain-only simulations were examined, the focus here will be put on snow-only simulations as the latter are much more scattering. Nonetheless, some conclusions drawn from the rain-only simulations are briefly discussed first.

The rain-only nadir simulations (not shown) presented very good consistency in the brightness temperatures simulated by RTTOV-SCATT, ARTS-MC and RT4 over both land and ocean emissivities for the highest accuracy settings (i.e., 30 nstreams in RT4 and 2400 min_iter in MC). The differences in the cloud signal, ie., the change in brightness temperatures between clear sky and scattering simulations (TB_{CLEAR} - TB_{CLOUDY}) simulated by RTTOV-SCATT and the two ARTS scattering modules were found to be less than 2 K for all channels. For the rain-only RT4 simulations, 10 nstreams were shown to achieve good simulations. Above 10 nstreams, increasing the number of nstreams in the simulations had very little impact over the performance, contrary to the minimum number of allowed iterations used in MC which has a significant impact; more than min_iter=1000 are needed to achieve good rain-only simulations. Finally, using different RT4 quadrature types showed to have little impact on the simulations.

Figure 5 shows the rain-only simulations discussed above as a function of observation angle. Similar results are obtained for land surface emissivities. As shown for clear sky simulations there is a degradation in the comparison of RTTOV and ARTS above 45 degrees. The nadir rain-only simulations were also analysed as a function of rain water level fraction (ifac). The rain water level fraction approach multiplies each level of the rain profile by ifac = 0 (i.e., clear sky), 0.5, 1.0, 1.5, 2.0, to analyse the sensitivity to the mass column. No impact was observed on the performance of these models with rain water column fraction (not shown). It should be noted however that a larger number of minimum iterations is required in the MC simulations.

As discussed in Section 3, the snow-only simulations were analysed following the soft sphere approach with mie theory and 3 habits from the DDA Liu [2008] database. As discussed for the rain-only simulations, the differences shown in RT4 simulations when using Gauss quadrature o Double Gauss quadrature are very small. Similarly to the rain-only simulations, the sensitivity to RT4 nstreams used is not strong, although a higher number of nstreams are needed for snow hydrometers than for rain (simulations here show that a minimum of 16 nstreams are needed to properly resolve the scattering matrix contrary to 4 for rain). Regarding min_iter, a value of 1600 shows to be sufficient to reach some sort of stability. The discussion so far regarding the snow-only simulation applies to both the soft sphere approach and the DDA habits.

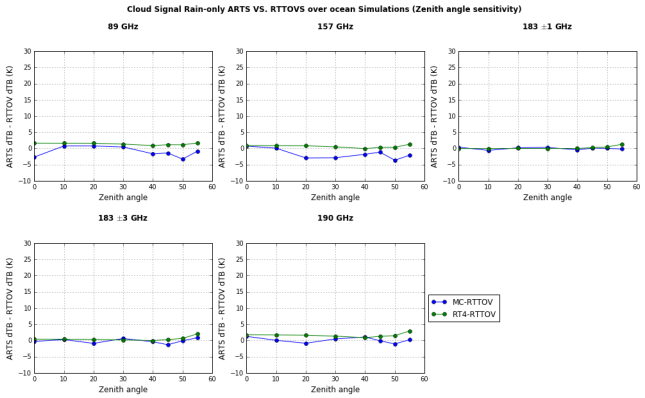

Figure 5: capition

Figure 6 shows the snow-only nadir ocean simulations for the highest accuracy settings (i.e., 30 nstreams in RT4 and 3000 min_iter in MC). The top panel shows the cloud signal for ARTS-MC (solid dotted lines), ARTS-RT4 (dashed lines) and RTTOV-SCATT (solid lines). The snow hydrometers in these simulations are modelled as soft spheres (using the Fabry and Szyrmer [1999] mixing formula) in blue, the DDA 6b ros. in red, the DDA dendrite in magenta and the DDA sector in cyan. As shown by the cloud signals modelled, these different snow hydrometers cover an interesting range of scattering properties; the soft sphere (6b. ros) being the least (most) scattering. The bottom panel shows the difference between the ARTS scattering simulations and RTTOV-SCATT (cloud signal difference). In general good consistency is achieved for these nadir simulations. In more detail, the largest differences are found at 89 GHz. For other frequency channels, differences between RTTOV-SCATT and the ARTS scattering modules range between -4 and 4 K. The larger differences at 89 GHz should be further explored, one possible improvement could be running MC simulations with higher min_iter values from the discussion above regarding min_iter. Note that in the case of the soft sphere approach, the Maxwell Garnett mixing formula [Garnett, 1904] was also tested in RTTOV and ARTS (not shown). The difference in the simulated cloud signals between RTTOV and the ARTS scattering modules was shown to be very similar for both mixing formulas analysed, only small differences were found at high observation angles at 89 GHz.

Figure 7 shows the difference in cloud signal between ARTS-MC, ARTS-RT4 and RTTOV-SCATT simulations as a function of zenith angle for ocean emissivities. As shown differences between RTTOV and ARTS increase with zenith angle for the soft sphere approximation (top panel), but for the DDA 6b. ros habit shown (bottom panel) the differences remain much more constant with zenith angle. A small increment can be shown for the higher slant angle observations, specially at 183±1 GHz, as shown for all simulations discussed so far. Similar results are shown for simulations over land (not shown), and for the other DDA habits explored. Note that the bottom panel shows that MC simula-

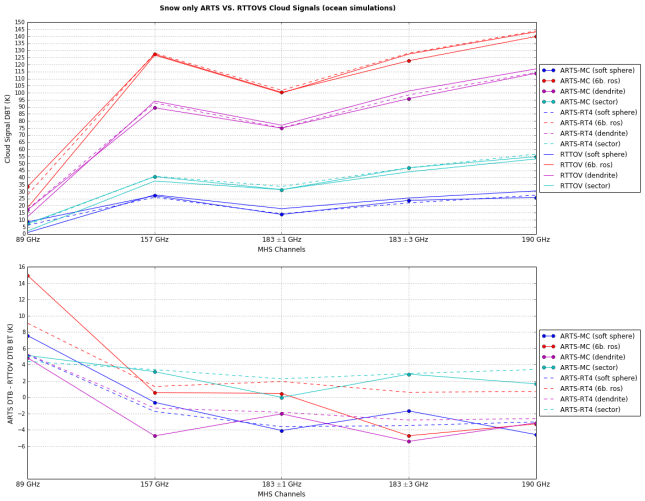

Figure 6: The cloud signal modelled by RTTOV and ARTS nadir ocean emissivity simulations using the RT4 (30 nstreams) and MC (min_iter=2500) scattering solvers for the snow-only profile from the Chevallier-91L deep-convection scenario. The soft sphere approximation and 3 habits from the DDA Liu [2008] database are tested.

tions should be run at larger min_iter as discussed above. The soft sphere approximation simulations requires further study, with differences between RTTOV-SCATT and ARTS as large as 25 K at 89 GHz and large slant angle observations. These differences in behaviour between the soft sphere approach and the DDA habit should be explored by analysing the phase function and the bulk asymmetry parameter. The phase function is a physical quantity that describes the angular distribution of the scattered energy, while the asymmetry parameter g describes the degree of symmetry of scattered energy distributed with respect to the plane dividing forward and backward hemispheres. The first Legendre moment of the phase function, is the asymmetry parameter g, and it represents the degree of asymmetry of the angular scattering. Higher g_{bulk} values mean a more complete forward direction and less angular scattering, while lower g means more isotropic scattering. This explains the different behaviour observed for simulations using Mie theory, which has higher g_{bulk} values at the frequencies explored versus the DDA habits as a function of zenith angle observation.

Finally, Figure 8 shows the difference in cloud signal between RTTOV and ARTS in the simulations shown in Figure 6 as a function of snow water level fraction (ifac) at nadir. The snow water level fraction approach multiplies each level of the snow profile by ifac = 0 (i.e., clear sky), 0.5, 1.0, 1.5, 1.0, to analyse the sensitivity to the mass column as done for the rain-only profile. The top panel shows the soft sphere approach and the bottom panel shows the DDA 6b. ros habit. Note that the other habits explored showed similar results and are not shown. No impact was observed in the comparison of the different radiative transfer models with increasing rain water column fraction. For the snow-only simulations

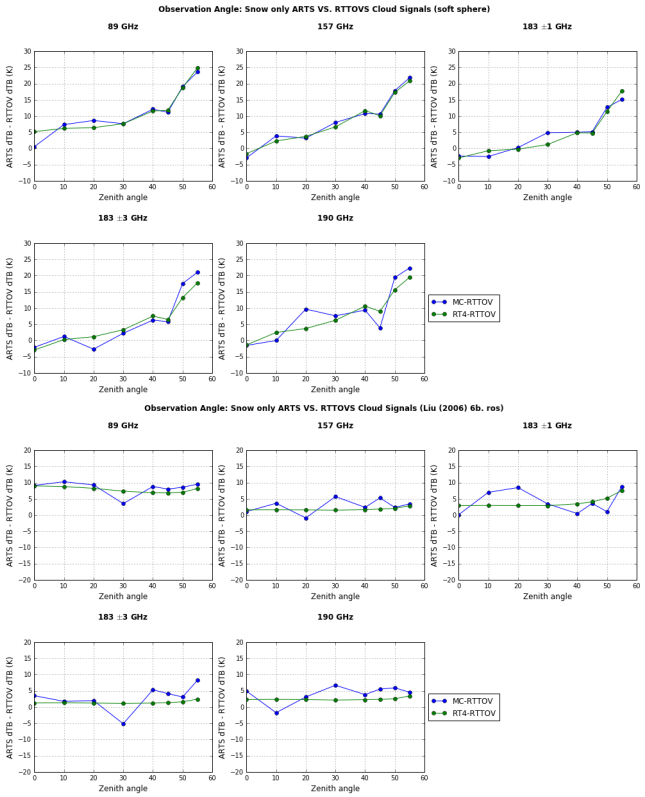

Figure 7: The difference between the cloud signal simulated by RTTOV and the different scattering solvers included in ARTS as a function of zenith angle for ocean emissivity simulations. The soft sphere approximation simulations are shown in the top panel, while the 6b. ros DDA habit is shown in the bottom panel.

using the soft sphere approach (top panel), there is also no sensitivity to increasing ifac either. Note that a different behaviour is observed on both top and bottom panels between the clear sky (ifac=0) and the cloudy ifac$\geq$0.5 simulations as expected. For the DDA 6b. ros habit, simulations show a strong dependence to ifac below 1. Note that, as discussed above, a higher number of min_iter settings are needed in MC simulations.

5 Summary and Future Work

This paper discusses ongoing work to compare the fast operational model RTTOV with the physics-based, research model, ARTS under cloudy conditions to intercompare their scattering solvers. It is important to develop an understanding of the systematic errors, or deficiencies, that may be presented in any given model. The simulations discussed in this paper correspond to simple scenarios where clear-sky, rain-only cloudy and snow-only cloudy conditions from a realistic deep convection case are modelled. These are simple, yet key comparisons that must be discussed before analysing more complex scenarios. The simulation discussed analyse the behaviour of the radiative transfer

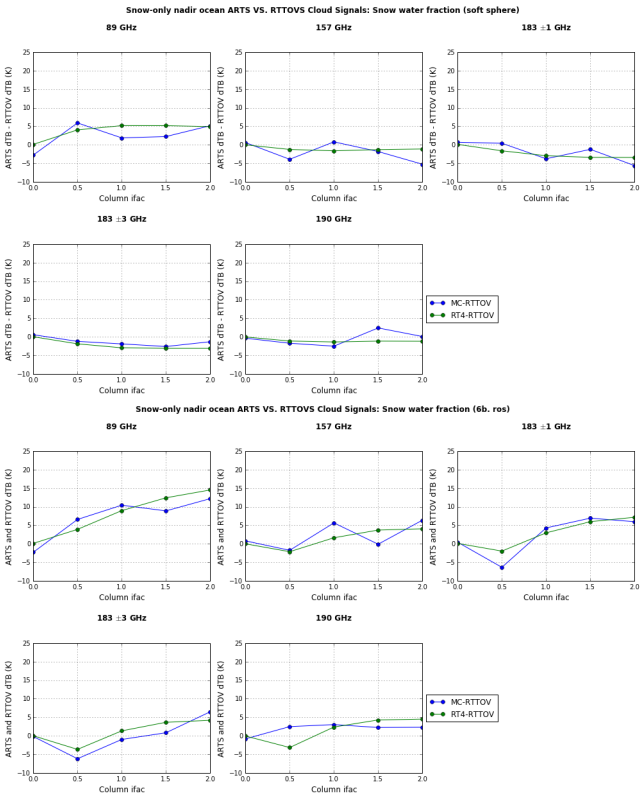

Figure 8: The difference between the cloud signal simulated by RTTOV and the different scattering solvers included in ARTS as a function of level snow mass content ifac for ocean emissivity simulations. The soft sphere approximation simulations are shown in the top panel, while the 6b. ros DDA habit is shown in the bottom panel. Similar results are obtained for land surface emissivities.

models to different parameters, such as the scattering properties, the zenith angle, or the cloud mass contents. Under clear sky conditions where both ARTS and RTTOV use the same water vapour absorption model, differences were shown to be below 1.5 K for nadir simulations. An analysis of the sensitivity of these simulations to zenith angle showed larger differences that need to be explored for zenith angles higher than $\sim$45 degrees. For cloudy conditions, the sensitivity of the ARTS simulations to MC min_iter, and RT4 nstreams and quadrature type were tested for rain-only and snow-only simulations, using the soft sphere approach and 3 habits from the Liu [2008] DDA databse for the latter. Using the soft-sphere approximation a strong sensitivity in the differences between RTTOV and ARTS cloud signals were shown as a function of zenith angle, but the these differences remain constant with snow water level fraction. The contrary is observed using DDA habits. There is no zenith angle sensitivity in the differences between RTTOV and ARTS, but there are differences as a function of snow water level fraction for all DDA habits, even the sector habit which has been shown to produce similar cloud signals to soft spheres (at 157 GHz 35 K cloud signals). This should being further explored by analysing the differences between these scattering solvers as a function of the scattering properties in a more systematic way. Further work is also being done to analyse the large differences found at 89 GHz simulations for the snow-only simulations.

Acknowledgements: Financial support to attend the International TOVS Study Conference-XXI from ATOVS/EUMETSAT

References

P. Bauer, E. Moreau, F. Chevallier, and U. O'Keefe. Multiple-scattering microwave radiative transfer for data assimilation applications. *Quart. J. Roy. Meteor. Soc.*, 132:1259–1281, 2006.

F. Chevallier, S. D. Michele, and A. McNally. Diverse profile datasets from the ecmwf 91-level short-range forecasts. Shinfield Park, Reading, December 2006.

C. P. Davis, D. L. Wu, C. Emde, J. H. Jiang, R. E. Cofield, and R. S. Harwood. Cirrus induced polarization in 122 ghz aura microwave limb sounder radiances. *Geophysical Research Letters*, 32(14), 2005.

P. Eriksson, S. Buehler, C. Davis, C. Emde, and O. Lemke. Arts, the atmospheric radiative transfer simulator, version 2. *Journal of Quantitative Spectroscopy and Radiative Transfer*, 112(10):1551 – 1558, 2011. ISSN 0022-4073.

K. F. Evans and G. L. Stephens. Microweve radiative transfer through clouds composed of realistically shaped ice crystals. part ii. remote sensing of ice clouds. *Journal of the Atmospheric Sciences*, 52(11):2058–2072, 1995.

J. Eyre. A fast radiative transfer model for satellite sounding systems. Shinfield Park, Reading, March 1991.

F. Fabry and W. Szyrmer. Modeling of the melting layer. part ii: Electromagnetic. *Journal of the Atmospheric Sciences*, 56(20):3593–3600, 1999.

M. Garnett. Colours in metal glasses and in metallic films. *Philosophical Transactions of the Royal Society of London A: Mathematical, Physical and Engineering Sciences*, 203(359-371):385–420, 1904. ISSN 0264-3952. doi: 10.1098/rsta.1904.0024.

A. J. Geer and F. Baordo. Improved scattering radiative transfer for frozen hydrometeors at microwave frequencies. *Atmospheric Measurement Techniques*, 7(6):1839–1860, 2014.

J. H. Joseph, W. J. Wiscombe, and J. A. Weinman. The delta-eddington approximation for radiative flux transfer. *Journal of the Atmospheric Sciences*, 33(12):2452–2459, 1976.

H. J. Liebe. Mpman atmospheric millimeter-wave propagation model. *International Journal of Infrared and Millimeter Waves*, 10(10), February 1989.

H. J. Liebe, G. A. Hufford, and M. G. Cotton, editors. *Propagation modeling of moist air and suspended water/ice particles at frequencies below 1000 GHz*, Nov. 1993.

G. Liu. A database of microwave single-scattering properties for nonspherical ice particles. *Bulletin of the American Meteorological Society*, 89(10):1563–1570, 2008.

P. W. Rosenkranz. Water vapor microwave continuum absorption: A comparison of measurements and models. *Radio Science*, 33(4):919–928, 1998.